© 2015. Published by The Company of Biologists Ltd | Journal of Cell Science (2015) 128, 4442-4452 doi:10.1242/jcs.180026

RESEARCH ARTICLE

$Ca_V3.2$ T-type channels mediate Ca^{2+} entry during oocyte maturation and following fertilization

Miranda L. Bernhardt[1], Yingpei Zhang[1], Christian F. Erxleben[2], Elizabeth Padilla-Banks[1], Caitlin E. McDonough[1], Yi-Liang Miao[3], David L. Armstrong[2] and Carmen J. Williams[1,*]

ABSTRACT

Initiation of mouse embryonic development depends upon a series of fertilization-induced rises in intracellular Ca^{2+}. Complete egg activation requires influx of extracellular Ca^{2+}; however, the channels that mediate this influx remain unknown. Here, we tested whether the α1 subunit of the T-type channel $Ca_V3.2$, encoded by *Cacna1h*, mediates Ca^{2+} entry into oocytes. We show that mouse eggs express a robust voltage-activated Ca^{2+} current that is completely absent in *Cacna1h*$^{-/-}$ eggs. *Cacna1h*$^{-/-}$ females have reduced litter sizes, and careful analysis of Ca^{2+} oscillation patterns in *Cacna1h*$^{-/-}$ eggs following *in vitro* fertilization (IVF) revealed reductions in first transient length and oscillation persistence. Total and endoplasmic reticulum (ER) Ca^{2+} stores were also reduced in *Cacna1h*$^{-/-}$ eggs. Pharmacological inhibition of $Ca_V3.2$ in wild-type CF-1 strain eggs using mibefradil or pimozide reduced Ca^{2+} store accumulation during oocyte maturation and reduced Ca^{2+} oscillation persistence, frequency and number following IVF. Overall, these data show that $Ca_V3.2$ T-type channels have prev8iously unrecognized roles in supporting the meiotic-maturation-associated increase in ER Ca^{2+} stores and mediating Ca^{2+} influx required for the activation of development.

KEY WORDS: Oocyte, Ca^{2+}, T-type channel, Meiosis, Fertilization, Egg activation

INTRODUCTION

The mammalian egg remains arrested at metaphase of the second meiotic division (MII) until fertilization triggers a series of oscillatory elevations in intracellular Ca^{2+} (Kline and Kline, 1992a; Miyazaki et al., 1986). These Ca^{2+} oscillations initiate a cascade of events referred to as egg activation, including resumption of the cell cycle, exocytosis of cortical granules and recruitment of maternal mRNAs for translation (Ducibella and Fissore, 2008; Schultz and Kopf, 1995). A transient increase in intracellular Ca^{2+} is a hallmark of fertilization in every animal species studied and is the primary driver of egg activation (Kashir et al., 2013; Stricker, 1999).

Several important changes occur during oocyte maturation to prepare the egg for proper Ca^{2+} mobilization upon fertilization. Growing oocytes within ovarian follicles remain arrested in meiotic prophase as germinal-vesicle-stage oocytes. Following the pre-ovulatory luteinizing hormone surge, Ca^{2+} levels increase within the oocyte endoplasmic reticulum (ER) as these cells progress through meiosis I and enter MII arrest (Cheon et al., 2013; Tombes et al., 1992). This increase in ER Ca^{2+} stores, rearrangement of the ER within the cell cortex, and increased expression of inositol trisphosphate (IP_3) receptors contribute to the enhanced Ca^{2+}-releasing ability of MII eggs compared to germinal vesicle oocytes (Fissore et al., 1999; FitzHarris et al., 2007; Mehlmann et al., 1996, 1995).

In addition to the importance of proper ER Ca^{2+} stores, extracellular Ca^{2+} is also required for sustained Ca^{2+} oscillations following fertilization (Igusa and Miyazaki, 1983; Kline and Kline, 1992b). We have previously shown that Ca^{2+} influx is required for full egg activation, as removal of Ca^{2+} from extracellular medium or broad inhibition of Ca^{2+} entry prevents emission of the second polar body (Miao et al., 2012). However, the Ca^{2+} channel or channels that mediate this Ca^{2+} influx have yet to be identified. Several studies have investigated the influence of store-operated Ca^{2+} entry (SOCE) or capacitative Ca^{2+} entry, a mechanism of Ca^{2+} influx activated in response to depletion of intracellular Ca^{2+} stores (Putney, 1986), in oocytes and eggs. Recent findings in mice suggest that Ca^{2+} influx through SOCE declines over oocyte maturation (Cheon et al., 2013), and treatment of fertilized eggs with SOCE inhibitors does not abate Ca^{2+} oscillations (Miao et al., 2012; Takahashi et al., 2013), supporting the proposition that alternative mechanisms of Ca^{2+} entry must be active at fertilization.

With the goal of determining the mechanism of SOCE-independent Ca^{2+} influx in mouse eggs, we tested the hypothesis that T-type channels contribute to Ca^{2+} entry following fertilization. In the studies presented here, we examined eggs from mice lacking the α1 subunit of $Ca_V3.2$ channels, CACNA1H, and investigated the effects of pharmacological inhibition of T-type channels. We show that $Ca_V3.2$ is the sole functional T-type channel in mouse eggs and is crucial both for proper Ca^{2+} store accumulation during oocyte maturation and for Ca^{2+} influx following fertilization to support sustained Ca^{2+} oscillations and full egg activation.

RESULTS

T-type channel α1 subunits, including CACNA1H and CACNA1I, are expressed in mouse oocytes and eggs

With the goal of identifying the ion channels that mediate Ca^{2+} influx following fertilization, we initially performed an *in silico* survey using publicly available microarray data (www.ncbi.nlm.nih.gov/geoprofiles) to determine which Ca^{2+}-permeable channels were likely to be expressed in mouse oocytes. From this list, we focused on low-threshold voltage-dependent T-type Ca^{2+} channels because the pore-forming α1 subunits for two of these channels, *Cacna1h* ($Ca_V3.2$) and *Cacna1i* ($Ca_V3.3$), appeared to have relatively high mRNA expression. To confirm these results and to define which related voltage-dependent Ca^{2+} channels could be present in oocytes and eggs, we quantified mRNA levels with real-time

[1]Reproductive and Developmental Biology Laboratory, National Institutes of Health, Research Triangle Park, NC 27709, USA. [2]Neurobiology Laboratory, National Institutes of Health, Research Triangle Park, NC 27709, USA. [3]Key Laboratory of Animal Genetics, Breeding, and Reproduction of Ministry of Education, College of Animal Science and Technology, Huazhong Agricultural University, Wuhan, 430070, China.

*Author for correspondence (williamsc5@niehs.nih.gov)

Received 4 September 2015; Accepted 12 October 2015

Journal of Cell Science (2015) 128, 4442-4452 doi:10.1242/jcs.180026

PCR. We identified three voltage-activated channels with mRNA levels significantly higher than the rest (Table 1): *Cacna1h* ($Ca_V3.2$), *Cacna1i* ($Ca_V3.3$) and the L-type channel *Cacna1d* ($Ca_V1.3$). Because *Cacna1h* mRNA was between twofold and eightfold more abundant than the other two in both oocytes and eggs (assuming similar primer efficiency), we focused on *Cacna1h* for further analysis.

$Ca_V3.2$ is the predominant functional T-type channel in mouse eggs

A mouse line with targeted disruption of *Cacna1h* has been generated previously (Chen et al., 2003). Whole-cell patch-clamp recordings were performed on eggs from *Cacna1h*$^{+/+}$, *Cacna1h*$^{+/-}$ and *Cacna1h*$^{-/-}$ mice. In *Cacna1h*$^{+/+}$ eggs, robust voltage-gated inward Ca^{2+} currents consistent with T-type channels were detected (Fig. 1A), similar to currents described in previous studies (Day et al., 1998; Kang et al., 2007; Peres, 1987). Voltage-gated Ca^{2+} current was reduced by 44% in *Cacna1h*$^{+/-}$ eggs compared to *Cacna1h*$^{+/+}$ and was undetectable in *Cacna1h*$^{-/-}$ eggs (Fig. 1A,B). Based on these results, $Ca_V3.2$ represents the only functional T-type Ca^{2+} channel present in mouse eggs. Addition of 10 µM pimozide or 10 µM mibefradil to bath solution also inhibited voltage-activated current in wild-type eggs (88% and 82% inhibition of maximum current, respectively), consistent with inhibition of T-type channels observed in previous studies (Kang et al., 2007; Martin et al., 2000; Williams et al., 1999). Current clamp mode was also used to measure resting membrane potential in wild-type eggs; values between −29 to −37 mV were observed before correction for junction potential, consistent with previous studies (Jaffe et al., 1983; Peres, 1986, 1987).

Cacna1h$^{-/-}$ females have reduced litter size

The *Cacna1h*$^{-/-}$ mouse line has been previously reported to be viable and fertile (Chen et al., 2003), but a formal breeding study has not been reported. To determine whether fertility was subtly impaired in this line, *Cacna1h*$^{+/+}$, *Cacna1h*$^{+/-}$ and *Cacna1h*$^{-/-}$ females were bred with wild-type C57Bl/6J males for 15 weeks; only data for the first three litters from pairs that produced at least three litters during this time were included for analysis. The time to first litter was not significantly different between the three groups (Fig. 1C), but *Cacna1h*$^{-/-}$ females had a significant reduction in the number of pups per litter compared to *Cacna1h*$^{+/+}$ females (Fig. 1D). Following superovulation, similar numbers of eggs were obtained from females of each genotype (26.8±3.9, 25.7±3.7, and 26.0±3.8 eggs for *Cacna1h*$^{+/+}$, *Cacna1h*$^{+/-}$, and *Cacna1h*$^{-/-}$, respectively, mean±s.e.m., n=6–8 mice/group); thus, the ovulatory response is apparently normal. Because *Cacna1h*$^{-/-}$ females are not infertile, $Ca_V3.2$ cannot be the sole ion channel capable of mediating Ca^{2+} influx in eggs. However, varying the level and duration of intracellular Ca^{2+} elevation following fertilization can substantially impact postimplantation embryo development even in the absence of effects on preimplantation development (Ozil et al., 2006, 2005), so we next investigated whether subtle disruption of Ca^{2+} signaling after fertilization could be a factor in the subfertility of *Cacna1h*$^{-/-}$ females.

Table 1. Expression of voltage-dependent Ca^{2+} channels in oocytes and eggs

Gene	Ca^{2+} channel	Germinal vesicle oocyte C_t	MII egg C_t
Cacna1s	$Ca_v1.1$	nd	nd
Cacna1c	$Ca_v1.2$	35.92±0.53	35.85±0.58
Cacna1d	$Ca_v1.3$	31.43±0.07	33.67±0.13
Cacna1f	$Ca_v1.4$	nd	nd
Cacna1a	$Ca_v2.1$	35.51±1.02	nd
Cacna1b	$Ca_v2.2$	34.34±0.02	34.29±0.19
Cacna1e	$Ca_v2.3$	34.86±0.11	35.87±0.15
Cacna1g	$Ca_v3.1$	nd	nd
Cacna1h	$Ca_v3.2$	28.66±0.23	30.87±0.08
Cacna1i	$Ca_v3.3$	31.07±0.19	32.77±0.13

Results are mean±s.e.m. C_t, threshold cycle; nd, not detected.

Cacna1h$^{-/-}$ eggs have a mild impairment in the Ca^{2+} response following IVF

Ratiometric Ca^{2+} imaging was performed on zona-pellucida-free *Cacna1h*$^{-/-}$ and *Cacna1h*$^{+/-}$ eggs during *in vitro* fertilization (IVF); representative traces are shown in Fig. 2A. Following insemination, eggs of both genotypes initiated Ca^{2+} oscillations, and oscillation frequency and amplitude were not significantly different (Fig. 2B,C). However, the length of the first Ca^{2+} transient of *Cacna1h*$^{-/-}$ eggs was significantly shorter than that of *Cacna1h*$^{+/-}$ eggs (Fig. 2D). Furthermore, the number of eggs with persistent Ca^{2+} oscillations during the first hour following IVF was significantly lower for *Cacna1h*$^{-/-}$ eggs compared to *Cacna1h*$^{+/-}$ eggs (Fig. 2E). To determine whether SOCE could compensate for lack of $Ca_V3.2$, IVF of *Cacna1h*$^{-/-}$ and *Cacna1h*$^{+/-}$ eggs was repeated in the presence of the SOCE inhibitor GSK1349571A (formerly called Synta66), previously shown to efficiently inhibit SOCE in mouse eggs (Miao et al., 2012). SOCE inhibition did not further reduce oscillation persistence or first transient length in *Cacna1h*$^{-/-}$ eggs (Fig. 2F–H), indicating that activation of SOCE did not provide a compensatory mechanism for Ca^{2+} uptake in *Cacna1h*$^{-/-}$ eggs.

Initial experiments were performed using only *Cacna1h*$^{-/-}$ and *Cacna1h*$^{+/-}$ eggs to simplify breeding. Because *Cacna1h*$^{+/-}$ eggs have reduced voltage-gated Ca^{2+} current relative to *Cacna1h*$^{+/+}$ eggs, IVF experiments were repeated using eggs from littermate *Cacna1h*$^{+/+}$ females to determine whether haploinsufficiency occurs in heterozygotes. Lower Ca^{2+} (0.5 mM) medium was also used in these experiments to test whether reducing the availability of extracellular Ca^{2+} impacted the *Cacna1h*$^{-/-}$ phenotype. The length and oscillation persistence of the first Ca^{2+} transient were significantly reduced in *Cacna1h*$^{-/-}$ eggs compared with both *Cacna1h*$^{+/-}$ and *Cacna1h*$^{+/+}$ (Fig. 2I,J). For both measurements, *Cacna1h*$^{+/-}$ values fell between those for *Cacna1h*$^{-/-}$ and *Cacna1h*$^{+/+}$, consistent with reduced $Ca_V3.2$ current in *Cacna1h*$^{+/-}$ eggs. Oscillation persistence and the length of the first Ca^{2+} transient was reduced for all genotypes in low Ca^{2+} (Fig. 2I) versus standard medium (Fig. 2D). To determine whether rates of polyspermy differed between groups, zona-pellucida-free eggs of each genotype were fertilized using similar conditions in parallel with eggs fertilized for imaging experiments, followed by fixation and DAPI staining. Similar low rates of polyspermy were found for each genotype (2 out of 27, 3 out of 25, and 4 out of 26 eggs with more than one sperm fused for *Cacna1h*$^{+/+}$, *Cacna1h*$^{+/-}$ and *Cacna1h*$^{-/-}$, respectively), indicating that the observed differences in Ca^{2+} oscillatory patterns do not result from differences in fertilization efficiency.

Ca^{2+} stores are reduced in *Cacna1h*$^{-/-}$ eggs

The finding that *Cacna1h*$^{-/-}$ eggs have shortened first Ca^{2+} transients following fertilization suggested that Ca^{2+} stores within the ER prior to fertilization might be lower, causing less Ca^{2+} to be available for release after fertilization. To test this idea, we assayed Ca^{2+} store content in *Cacna1h*$^{-/-}$ eggs. To compare total cellular

Journal of Cell Science (2015) 128, 4442-4452 doi:10.1242/jcs.180026

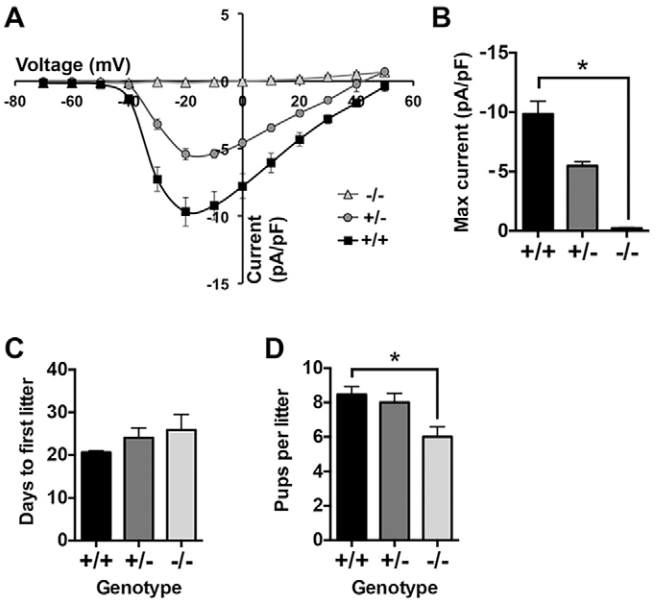

Fig. 1. *Cacna1h*$^{-/-}$ eggs lack T-type Ca^{2+} currents, and *Cacna1h*$^{-/-}$ females are subfertile. (A,B) Whole-cell recordings were performed in the presence of 20 mM extracellular Ca^{2+}. Current–voltage (*I–V*) relationship and maximum current are graphed for each genotype (n=9, 3 or 11 eggs from three *Cacna1h*$^{+/+}$, one *Cacna1h*$^{+/-}$ and three *Cacna1h*$^{-/-}$ mice, respectively). *P<0.05 (Kruskal–Wallis test with Dunn's multiple comparison test). *Cacna1h*$^{+/+}$, *Cacna1h*$^{+/-}$ and *Cacna1h*$^{-/-}$ females were bred with wild-type C57BL/6J males for 15 weeks. (C) Time to first litter in days (n=5–6 pairs per genotype). Results are not significantly different (Kruskal–Wallis test). (D) Graph of average number of pups per litter (n=15–18 litters per genotype). *P<0.05 (Kruskal–Wallis test with Dunn's multiple comparison). Results are mean±s.e.m.

Ca^{2+} stores, ionomycin-induced Ca^{2+} release was measured for *Cacna1h*$^{-/-}$ and *Cacna1h*$^{+/-}$ eggs. Both area under the curve and maximum amplitude of the Ca^{2+} release were slightly but significantly reduced in *Cacna1h*$^{-/-}$ eggs relative to *Cacna1h*$^{+/-}$ eggs (Fig. 3A–C). To determine whether the difference in total store content was present prior to oocyte maturation, this assay was repeated on germinal-vesicle-stage *Cacna1h*$^{-/-}$ and *Cacna1h*$^{+/-}$ oocytes. No significant difference in germinal vesicle oocyte total Ca^{2+} stores was observed (Fig. 3D–F), indicating that *Cacna1h*$^{-/-}$ oocytes accrue less Ca^{2+} during oocyte maturation.

To more directly measure ER Ca^{2+} stores, Ca^{2+} release following addition of the sarco-endoplasmic reticulum Ca^{2+} ATPase inhibitor, thapsigargin, was measured over the course of oocyte maturation. Germinal vesicle oocytes were collected from ovaries of pregnant mare's serum gonadotropin (PMSG)-primed mice of each genotype and a subset were matured *in vitro* to obtain germinal vesicle breakdown (GVBD) and metaphase I (MI) stage oocytes; ovulated MII eggs were collected from oviducts following superovulation. Oocytes and eggs from wild-type *Cacna1h*$^{+/+}$ littermates were also included for these assays. ER Ca^{2+} stores for all three genotypes increased between the germinal vesicle and MI stage; however, although levels continued to rise during the MI–MII transition in *Cacna1h*$^{+/+}$ and *Cacna1h*$^{+/-}$ oocytes, ER Ca^{2+} did not increase between MI and MII in *Cacna1h*$^{-/-}$ oocytes, such that ER Ca^{2+} stores in *Cacna1h*$^{-/-}$ MII eggs were reduced by nearly 70% compared to levels in *Cacna1h*$^{+/+}$ eggs (Fig. 3G–I). ER Ca^{2+} content of *Cacna1h*$^{-/-}$ germinal vesicle oocytes was reduced by ~40% relative to *Cacna1h*$^{+/+}$ germinal vesicle oocytes (Fig. 3H,I), indicating that $Ca_V3.2$ might also play a role in maintaining oocyte Ca^{2+} homeostasis prior to meiotic maturation. Taken together, these results show that $Ca_V3.2$ is crucial for appropriate accrual of the ER Ca^{2+} stores required for a normal Ca^{2+} response at fertilization.

Pharmacological inhibition of $Ca_V3.2$ during *in vitro* maturation reduces ER Ca^{2+} store content

To determine whether $Ca_V3.2$ supports Ca^{2+} influx during maturation in another mouse strain, wild-type CF-1 oocytes were matured *in vitro* in the presence of T-type channel inhibitors, and ER Ca^{2+} stores were assayed. When germinal vesicle oocytes were matured in the presence of 10 µM mibefradil, fewer cells reached the MII stage, with 49% of mibefradil-treated oocytes arresting at GVBD or MI, compared to 12% of controls. This result is consistent with the requirement for extracellular Ca^{2+} for meiotic division (Homa et al., 1993; Jagiello et al., 1982; Tombes et al., 1992). Germinal vesicle oocytes matured in the presence of 1–5 µM mibefradil progressed normally to MII (92%, 95% and 96% of cells cultured in 0, 1 and 5 µM mibefradil, respectively, produced first polar bodies). Thapsigargin-induced Ca^{2+} release was measured for these mibefradil-treated MII eggs and was significantly reduced, indicating reduced ER Ca^{2+} store content (Fig. 4A–C). Baseline Ca^{2+} signal, reflected by ratio of fluorescence at 340 nm to that at 380 nm (F340/F380) in fura-2 AM-loaded cells, was also notably lower in MII eggs following maturation in the presence of mibefradil (Fig. 4D). Oocytes were also treated with a second T-type channel inhibitor, pimozide. Oocytes matured in 0.5, 2, and 5 µM pimozide all had significantly reduced ER Ca^{2+} content (Fig. 4E–G). Concentrations of pimozide of 5 µM or lower did not impair oocyte maturation to MII (89% of controls and an average of 96% of pimozide-treated oocytes divided to produce first polar bodies), and pimozide had a less substantial impact on baseline Ca^{2+} signal than mibefradil, with only eggs cultured in the lowest concentration of pimozide showing a small but statistically significant reduction in the baseline signal (Fig. 4H). The reductions in ER store content are unlikely to be the result of non-specific toxicity, because oocytes only began to show any signs of toxicity, such as visible changes in appearance of the cytoplasm, after 15–16 h of culture in 10 µM mibefradil or 20 µM pimozide. Overall, these data are consistent with Ca^{2+} store measurements in *Cacna1h*$^{-/-}$ eggs, suggesting reduction in ER Ca^{2+} stores in these mice directly results from loss of $Ca_V3.2$ activity.

Inhibition of $Ca_V3.2$ during IVF impairs Ca^{2+} oscillations and reduces constitutive divalent cation influx in MII eggs

Reduced Ca^{2+} oscillation persistence in *Cacna1h*$^{-/-}$ eggs suggested that $Ca_V3.2$ channels contribute to Ca^{2+} influx required for sustained Ca^{2+} oscillations. To further investigate this role, wild-type CF-1 strain eggs were cultured in the presence of 10 µM mibefradil or 5 µM pimozide during IVF, and Ca^{2+} oscillation patterns were analyzed. Prior to insemination, eggs were incubated in BSA-free medium in the presence or absence of each inhibitor for 15–30 min. Presence of either inhibitor substantially impaired Ca^{2+} oscillations (Fig. 5). Oscillation frequency was significantly decreased, as was the length of the first transient (Fig. 5B,C,H,I). Pimozide, but not mibefradil, also reduced the amplitude of the first Ca^{2+} transient (Fig. 5D,J). Oscillation persistence during the first 60 min after insemination was markedly reduced in the presence of either inhibitor (Fig. 5E,K), which was also reflected by a significant reduction in the number of oscillations during imaging (Fig. 5F,L). This result strongly implicates mibefradil- and pimozide-sensitive channels as a primary means of Ca^{2+} influx required for sustained Ca^{2+} oscillations after fertilization.

Journal of Cell Science (2015) 128, 4442-4452 doi:10.1242/jcs.180026

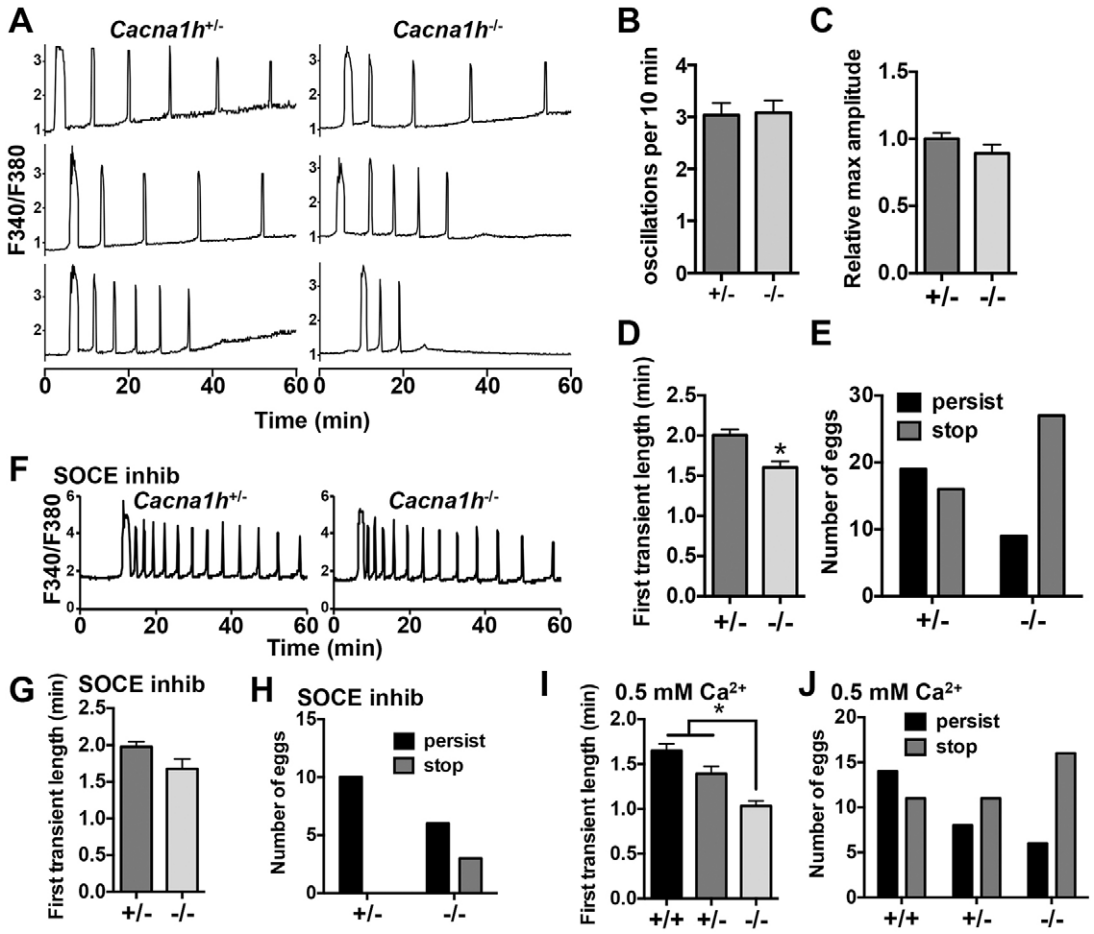

Fig. 2. Ca^{2+} oscillation pattern following IVF for *Cacna1h*$^{-/-}$ eggs. Ratiometric Ca^{2+} imaging of *Cacna1h*$^{+/-}$ and *Cacna1h*$^{-/-}$ eggs was performed during IVF. (A) Representative traces are shown. (B,C) Graphs show oscillation frequency and relative maximum amplitude (n=22–24 eggs per genotype over three replicate experiments). Results are not significantly different (Mann–Whitney test). (D) First transient length in minutes (n=36–37 eggs per genotype over seven replicate experiments). *P<0.05 (Mann–Whitney test). (E) Persistence of oscillations to the end of the 60-min imaging period differed significantly between genotypes (P<0.05, Fisher's exact test, n=35–36 eggs per genotype over seven replicate experiments). (F–H) IVF experiments were repeated with addition of 2 µM GSK1349571A (SOCE inhibitor) to the imaging medium; representative traces and graphs of first transient length and oscillation persistence are shown (n=9–12 eggs per genotype over three replicate experiments). Results are not significantly different (Mann–Whitney and Fisher's exact test). (I,J) IVF experiments were performed in low-Ca^{2+} medium (0.5 mM) with *Cacna1h*$^{+/+}$, *Cacna1h*$^{+/-}$, and *Cacna1h*$^{-/-}$ eggs; graphs of first transient length and oscillation persistence are shown (n=19–25 eggs per genotype over five replicate experiments). *P<0.05 (Kruskal-Wallis with Dunn's multiple comparison test) in I; and P<0.05 in J (χ-square test for trend). Results are mean±s.e.m.

To measure constitutive divalent cation influx as an indicator of Ca^{2+} entry, fura-2 quenching by Mn^{2+} was determined by imaging at 360 nm (F360; the Ca^{2+} isosbestic point for fura-2) in unfertilized MII eggs (Bird et al., 2008; McGuinness et al., 1996). Eggs were cultured in medium containing 1.8 mM Ca^{2+} during imaging as 1 mM Mn^{2+} was added. Minimum fluorescence (F_{min}) was determined by adding ionomycin ~15 min after Mn^{2+} addition, and imaging was continued for 10 min. Following normalization to the initial baseline and F_{min}, the decrease in F360 from 2 to 7 min after Mn^{2+} addition was determined. A trend toward reduction in rate of fluorescence loss was noted with culture in 5 µM pimozide, and a significant reduction was observed with 10 µM pimozide (Fig. 6A,B). Using 10–50 µM mibefradil in similar assays, we were unable to detect inhibition of constitutive divalent cation influx (not shown); this finding might indicate that additional channels or other pathways inhibited by pimozide but not mibefradil contribute to constitutive influx. In all, these results support the conclusion that $Ca_V3.2$ is a key mediator of Ca^{2+} influx in mouse eggs, both before and after fertilization.

DISCUSSION

Ca^{2+} is a crucial driver of the activation of embryonic development, and influx of extracellular Ca^{2+} is required for sustained Ca^{2+} oscillations and complete egg activation in mice (Igusa and Miyazaki, 1983; Kline and Kline, 1992a,b; Miao et al., 2012; Runft et al., 2002). In this study, we interrogated the role of the T-type Ca^{2+} channel $Ca_V3.2$ in mediating Ca^{2+} entry during oocyte maturation and following fertilization. We demonstrate that mice lacking the pore-forming subunit of $Ca_V3.2$, CACNA1H, have slightly impaired fertility and produce eggs with undetectable voltage-gated Ca^{2+} current, reduced ER Ca^{2+} store content, shortened first Ca^{2+} transients following IVF and reduced Ca^{2+} oscillation persistence. We also show that inhibition of $Ca_V3.2$ with mibefradil or pimozide during meiotic maturation recapitulates the reduction in ER Ca^{2+} stores, and treatment with either inhibitor during IVF leads to an even greater impairment of Ca^{2+} oscillations than loss of CACNA1H alone, suggesting that additional Ca^{2+} entry mechanisms mediate partial compensation in *Cacna1h*$^{-/-}$ eggs. Taken together, these results support a model in which the T-type

Journal of Cell Science (2015) 128, 4442-4452 doi:10.1242/jcs.180026

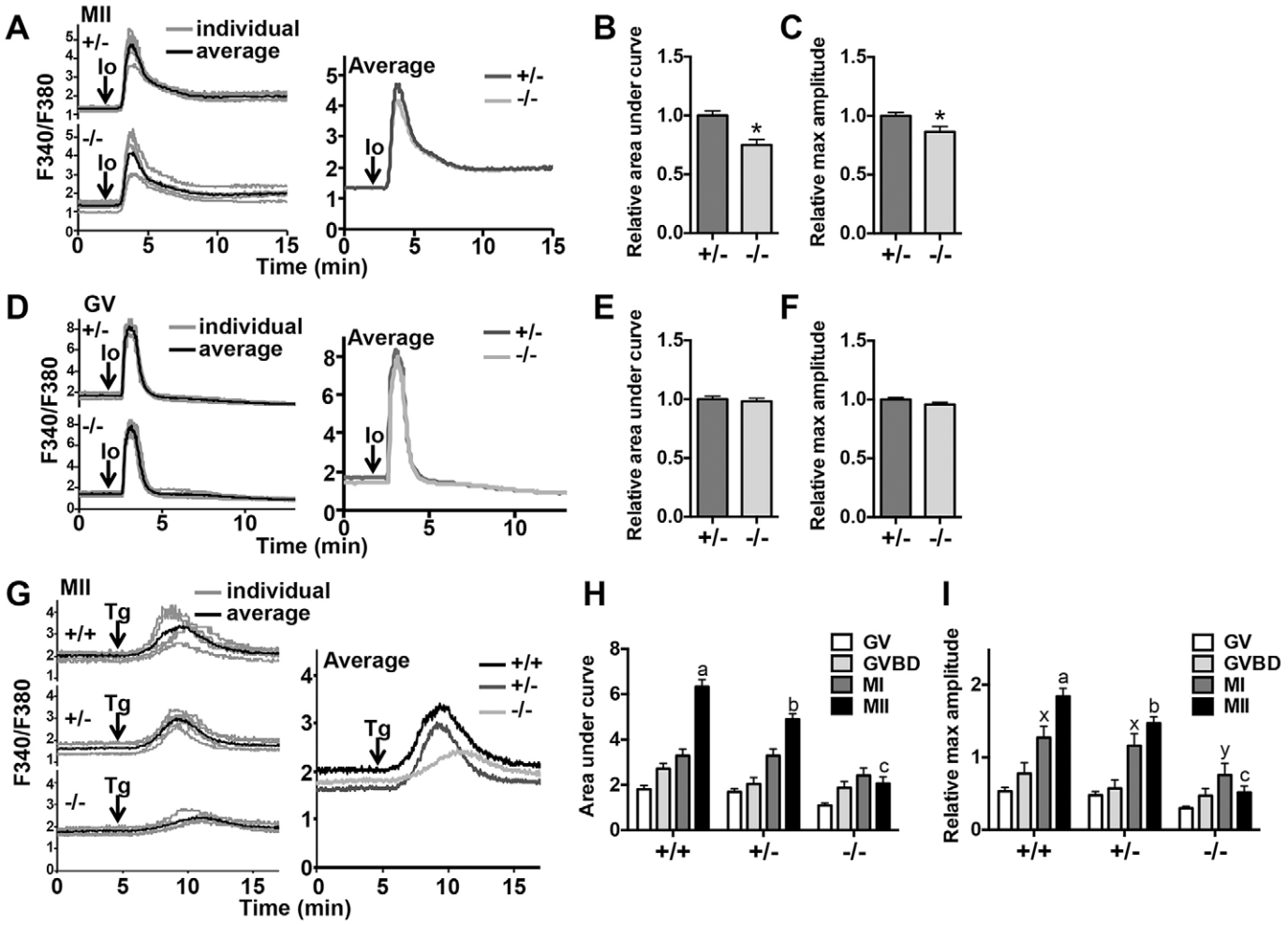

Fig. 3. Total and ER Ca^{2+} stores are reduced in *Cacna1h*$^{-/-}$ eggs and maturing oocytes. Ionomycin-induced Ca^{2+} release was measured for *Cacna1h*$^{+/-}$ and *Cacna1h*$^{-/-}$ eggs and germinal vesicle (GV) oocytes. (A,D) Representative curves are shown for individual eggs or oocytes (gray lines) and as averages for 5–6 cells (black lines); average traces for both genotypes are also shown on the same graph for comparison. (B,C) Area under the curve and maximum amplitude were graphed for MII eggs (n=21 eggs per genotype over four replicate experiments). *P<0.05 (unpaired t-test with Welch's correction). (E,F) Graphs of area under the curve and maximum amplitude for germinal vesicle oocytes (n=44–50 oocytes per genotype from eight replicate experiments). Results are not significantly different (unpaired t-test with Welch's correction). (G) Representative traces of thapsigargin-induced Ca^{2+} release for individual MII eggs (gray lines) and averages for five eggs (black lines) are shown, along with compiled averages on one graph. (H,I) Area under the curve and maximum amplitude relative to baseline are graphed for *Cacna1h*$^{+/+}$, *Cacna1h*$^{+/-}$ and *Cacna1h*$^{-/-}$ MII eggs and IVM oocytes. GVBD oocytes were assayed after 2.5 h of IVM, MI oocytes after 5.75–6.5 h IVM, and MII eggs at 15.5–17.5 h after hCG administration. 12–25 oocytes or eggs were assayed per genotype over three to five experimental replicates for each developmental stage. $^{a,b,c,x,y}P$<0.05 (two-way ANOVA with Tukey's multiple comparison test; different letters show significant differences between genotypes for each developmental time point). Io, ionomycin; Tg, thapsigargin. Results are mean±s.e.m.

channel $Ca_V3.2$ contributes to Ca^{2+} influx during oocyte maturation to support the accumulation of ER Ca^{2+} that prepares the egg for fertilization as well as the Ca^{2+} influx necessary to sustain Ca^{2+} oscillations after fertilization (summarized in Fig. 7).

Ca^{2+} oscillations following fertilization depend upon ER Ca^{2+} stores. Phospholipase Cζ delivered by the fertilizing sperm causes hydrolysis of egg phosphatidylinositol (4,5)-bisphosphate to produce diacylglycerol and IP_3; IP_3 then acts on IP_3 receptors in the ER to induce Ca^{2+} release (Kashir et al., 2014; Saunders et al., 2002). With each Ca^{2+} release, reduction in Ca^{2+} levels within the ER is observed (Takahashi et al., 2013; Wakai and Fissore, 2013), and there is evidence of Ca^{2+} entry concurrent with initial Ca^{2+} transients following fertilization (McGuinness et al., 1996). Based on these observations, SOCE, which relies upon detection of low ER Ca^{2+} by STIM1 and STIM2 proteins, which promote Ca^{2+} influx through ORAI channels (reviewed in Bird et al., 2008; Putney, 2007), might be considered a prime candidate for mediating the Ca^{2+} influx needed to sustain Ca^{2+} oscillations in mammalian eggs. Although SOCE components are present in mouse oocytes and eggs (Cheon et al., 2013; Miao and Williams, 2012), and previous reports have suggested that SOCE might be active during mammalian oocyte maturation and fertilization (Cheon et al., 2013; Gomez-Fernandez et al., 2012, 2009; Lee et al., 2012; Wang et al., 2012, 2015), evidence against a requisite role for SOCE is also mounting. We have previously shown that chemical inhibition of SOCE following fertilization does not impair Ca^{2+} oscillations or egg activation events (Miao et al., 2012). Consistent with these findings, expression of protein fragments that inhibit STIM1–ORAI1 interactions does not inhibit fertilization-induced Ca^{2+} oscillations (Takahashi et al., 2013). Other reports have also suggested that SOCE is low or becomes inactivated during mouse and *Xenopus* oocyte maturation and during mitotic division in mammalian cells (Cheon et al., 2013; Machaca and Haun, 2002; Smyth et al., 2009). These results led us to focus on SOCE-

Journal of Cell Science (2015) 128, 4442-4452 doi:10.1242/jcs.180026

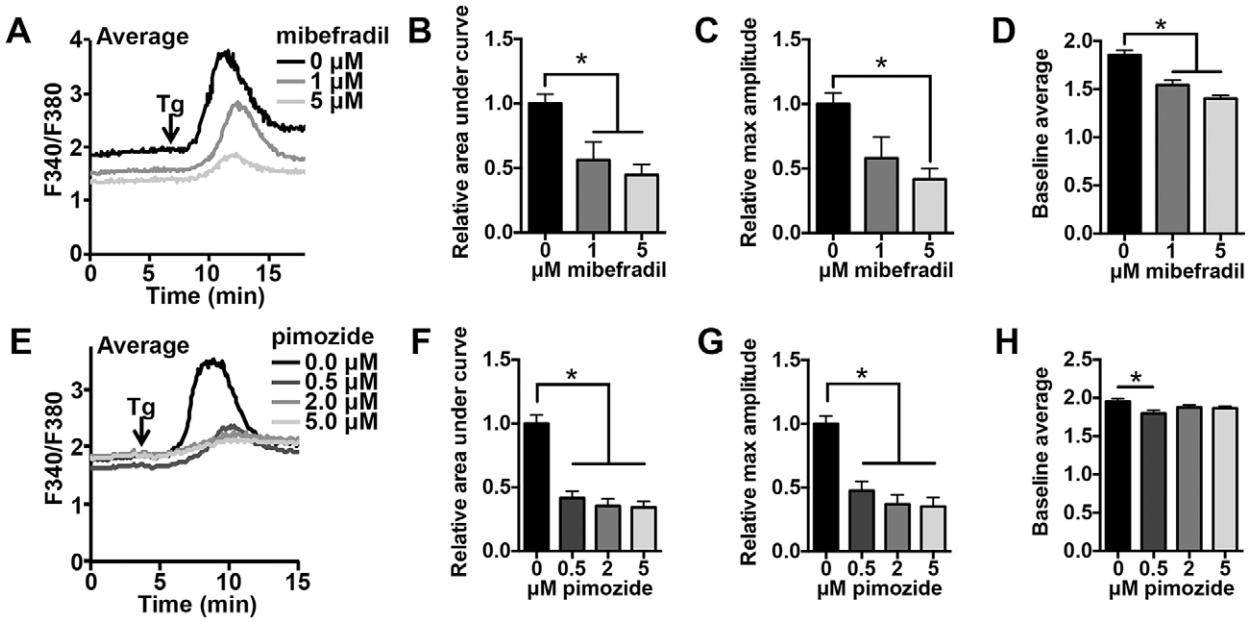

Fig. 4. Inhibition of T-type channels during *in vitro* maturation impairs ER Ca^{2+} store accumulation. Germinal-vesicle-stage oocytes were collected and matured *in vitro* in the presence or absence of T-type channel inhibitors, mibefradil and pimozide. (A) Representative thapsigargin-induced Ca^{2+} release curves are shown for oocytes matured in 0, 1 or 5 µM mibefradil; each trace shows average data for 4–5 MII eggs. (B–D) Graphs of relative area under the curve, maximum amplitude relative to baseline and average baseline are shown (n=8–9 eggs per treatment from two experimental replicates). *P<0.05 (one-way ANOVA with Tukey's multiple comparison test). (E) Representative average Ca^{2+} traces from 4-5 MII eggs matured in 0, 0.5, 2, or 5 µM pimozide are shown. (F-H) Graphs of relative area under the curve, maximum amplitude relative to baseline and average baseline are shown (n=16–18 eggs per treatment from four experimental replicates). *P<0.05 (Kruskal-Wallis with Dunn's multiple comparison test). All assays were performed after 14.5–17.5 h IVM. Tg, thapsigargin. Results are mean±s.e.m.

independent modes of Ca^{2+} entry as possible mediators of Ca^{2+} influx in oocytes and eggs.

Cacna1h$^{-/-}$ eggs had short first Ca^{2+} transients, which we hypothesized could reflect an underlying reduction in ER Ca^{2+} stores. Increase in ER Ca^{2+} store capacity occurs during oocyte maturation and is thought to be part of the preparation for fertilization by the egg (Cheon et al., 2013; Tombes et al., 1992). Based on the data shown here, $Ca_V3.2$ is a key mediator of this Ca^{2+} accumulation process. Total Ca^{2+} store content, assayed by measuring Ca^{2+} release following ionomycin treatment, was slightly reduced in *Cacna1h*$^{-/-}$ MII eggs but not germinal vesicle oocytes, indicating that $Ca_V3.2$ is needed for normal Ca^{2+} accrual during oocyte maturation. Thapsigargin-mediated Ca^{2+} release, used as a measure of ER Ca^{2+} store content, was dramatically reduced in both *Cacna1h*$^{-/-}$ MII eggs and germinal vesicle oocytes, and this phenotype was recapitulated by maturing wild-type oocytes in the presence of mibefradil or pimozide. ER Ca^{2+} stores were reduced at inhibitor concentrations that did not inhibit oocyte maturation; however, higher concentrations (10 µM mibefradil or 20 µM pimozide) reduced rates of first polar body emission, consistent with previous studies showing that extracellular Ca^{2+} is required for progression beyond MI (Homa et al., 1993; Jagiello et al., 1982; Tombes et al., 1992). This result indicates that ER store accumulation is more sensitive to reduced T-type channel activity than progression through MI, or that additional channels or cellular targets sensitive to higher concentrations of these inhibitors also contribute to meiotic progression. Mouse eggs contain both thapsigargin-sensitive and -insensitive Ca^{2+} stores (Kline and Kline, 1992b). The more dramatic reduction in ER Ca^{2+} compared to total Ca^{2+} suggests that accrual of the thapsigargin-sensitive pool of ER Ca^{2+} is particularly sensitive to loss of $Ca_V3.2$.

Both genetic loss of *Cacna1h* and treatment with T-type channel inhibitors impaired oscillation persistence following IVF. Because disruption of Ca^{2+} oscillation patterns caused by pharmacological inhibition was more severe than that caused by loss of $Ca_V3.2$ alone, it is likely that additional voltage-independent channels blocked by pimozide or mibefradil also contribute to Ca^{2+} entry following fertilization and/or that additional compensatory mechanisms are active in *Cacna1h*$^{-/-}$ eggs. Using real-time PCR, we detected appreciable levels of a second T-type channel subunit, *Cacna1i* ($Ca_V3.3$), and one L-type subunit, *Cacna1d* ($Ca_V1.3$). Based on our electrophysiology data, however, no voltage-dependent Ca^{2+} current is detectable in eggs lacking $Ca_V3.2$; therefore $Ca_V3.3$ and $Ca_V1.3$ are unlikely to contribute to Ca^{2+} entry. Furthermore, inhibitor concentrations used were below the IC_{50} for L-type channels for pimozide and near or below the L-type IC_{50} for mibefradil (Kuryshev et al., 2014), and no effects on Ca^{2+} oscillations or Ca^{2+} currents were observed with addition of the L-type channel activator Bay K6844 (data not shown), providing further support for the conclusion that functional L-type channels are not present in mouse eggs. The significant decrease in oscillation frequency observed following T-type inhibitor treatment is consistent with previous data showing that oscillation frequency is dependent upon the rate of Ca^{2+} influx (Takahashi et al., 2013). Importantly, we found that pre-incubation of eggs in BSA-free medium in the presence of either pimozide or mibefradil for 15–30 min prior to fertilization was crucial for a strong impact on oscillation persistence to be observed. This requirement might be related to the relatively slow inhibitor binding rate described for pimozide (Arnoult et al., 1998) or to BSA binding the inhibitors or otherwise reducing their effects. Lack of an effect of pimozide on fertilization-induced Ca^{2+} oscillations has been mentioned previously (McGuinness et al., 1996); however, exact

Journal of Cell Science (2015) 128, 4442-4452 doi:10.1242/jcs.180026

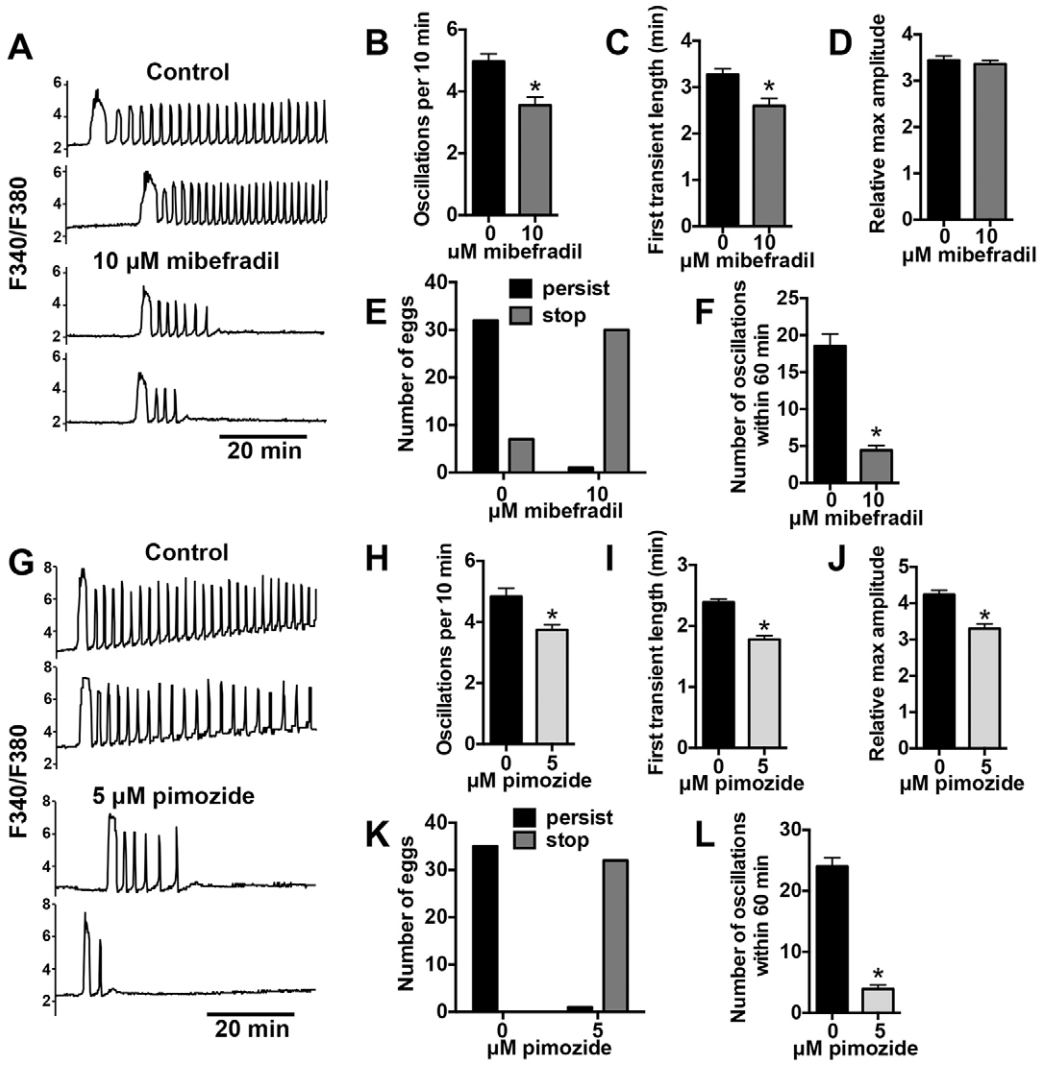

Fig. 5. Inhibition of T-type channels impairs Ca^{2+} oscillations following IVF. Wild-type CF-1 eggs were fertilized *in vitro* in the presence of mibefradil, pimozide or vehicle control. (A,G) Representative traces of Ca^{2+} response following IVF are shown. (B–F,H–L) Ca^{2+} oscillation parameters and persistence to the end of the 60-min imaging period are graphed as indicated (n=29–38 eggs per treatment over three replicate experiments). *P<0.05 for B–C, F, H–J and L (unpaired t-test with Welch's correction or Mann-Whitney, as appropriate), and oscillation persistence between treatments was significantly different in E and K (P<0.05, Fisher's exact test).

experimental conditions were not stated. Differences in media constituents or the presence of BSA might explain this discrepancy. *Cacna1h*$^{-/-}$ females are not completely infertile, thus additional channels must be capable of supporting the Ca^{2+} influx needed to sustain Ca^{2+} oscillations. Further studies are underway to test the roles of voltage-independent Ca^{2+} entry mechanisms in mouse oocytes and eggs.

In contrast to many invertebrate species, in which sperm–egg fusion results in membrane depolarization thought to inhibit polyspermy (Gould-Somero et al., 1979), fertilization in mammals appears to be accompanied by only a small change in membrane potential (Igusa et al., 1983; Jaffe et al., 1983). For this reason, it might be surprising that voltage-dependent channels are functional in mouse oocytes and eggs. However, voltage-dependent Ca^{2+} channel actions in non-excitable cells are not without precedent. Ca^{2+} influx currents consistent with T-type channels have been measured previously in mouse eggs (Day et al., 1998; Kang et al., 2007; Peres, 1987). T-type channels are also important during oocyte growth and maturation in ascidians (Gallo et al., 2013), indicating that the role of these channels might be conserved. In addition, T-type channels are important for sperm function (Arnoult et al., 1996, 1998; Darszon et al., 2006). Furthermore, a variety of cellular effectors can modulate T-type channel activity (reviewed in Zhang et al., 2013), including CaMKIIγ (Kang et al., 2007), which is a direct downstream effector of the Ca^{2+} signal at fertilization and mediates many events of egg activation (Backs et al., 2010; Knott et al., 2006; Markoulaki et al., 2003).

Certain types of Ca^{2+} channels, including T-type, display persistent inward currents at low voltages, referred to as 'window currents' (Williams et al., 1997; reviewed in Capiod, 2011). These currents are mediated by partial channel activation combined with incomplete inactivation at voltages between those producing maximal activation and complete steady-state inactivation, resulting in a small proportion of active channels that sustain inward Ca^{2+} currents (Capiod, 2011; Chemin et al., 2000; Serrano et al., 1999; Williams et al., 1997). In various cell types, window currents can occur at or near the resting membrane potential. In cells of the embryonic mouse hindbrain, window current occurs in the range of −6 to −46 mV, peaking at −31 mV (Watari et al., 2014). Predicted window currents in HEK293 cells overexpressing

Journal of Cell Science (2015) 128, 4442-4452 doi:10.1242/jcs.180026

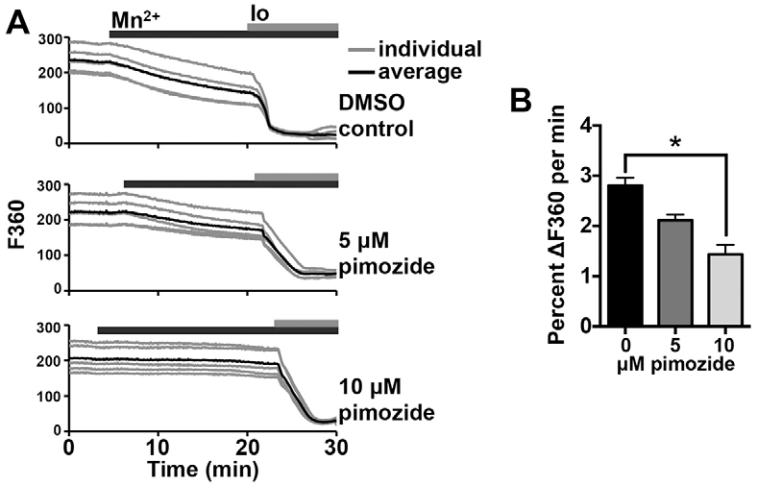

Fig. 6. Inhibition of T-type channels reduces constitutive divalent cation influx. Mn^{2+}-quenching assays were performed using fura-2-AM-loaded MII eggs. (A) Representative graphs of F360 are shown for individual eggs (gray lines) and averages for five eggs (black lines). Top panel, DMSO control; middle panel, 5 µM pimozide; bottom panel, 10 µM pimozide. (B) The rate of decrease in F360 from min 2–7 following Mn^{2+} addition, relative to baseline fluorescence and minimum fluorescence level within 10 min after ionomycin addition, is shown (n=23–36 eggs over 2–3 replicate experiments per treatment). *P<0.05 (Kruskal–Wallis with Dunn's multiple comparison test). Io, ionomycin. Results are mean±s.e.m.

Cacna1h and *Cacna1g* peak at −65 and −48 mV, respectively (Chemin et al., 2000). Resting membrane potential in these cells was measured as −35 mV, suggesting that the expressed channels could permit moderate and constant Ca^{2+} entry at resting membrane potential (Chemin et al., 2000). In unfertilized mouse eggs, resting membrane potential has been measured at −41 mV to −18 mV (Jaffe et al., 1983; Peres, 1986, 1987; and data presented here). Thus, the resting membrane potential of mouse eggs is well within the range of voltages that support Ca^{2+} influx through window current activity in other cell types. For $Ca_V3.1$ channels, inactivation is incomplete at all membrane potentials, leaving 1–2% of channels open and capable of conducting current (Serrano et al., 1999). We postulate that window current supported by $Ca_V3.2$ channels mediates Ca^{2+} influx in mouse oocytes and eggs.

Although the exact mechanism of T-type channel regulation in mouse oocytes and eggs requires further elucidation, it is clear that genetic loss of *Cacna1h* impacts upon Ca^{2+} homeostasis and dynamics; therefore, $Ca_V3.2$ must be functional in these cells. Window currents provide a plausible explanation for T-type channel activation in non-excitable cells, but several important caveats must be considered, including methods used for determining the true resting membrane potential of eggs, membrane potential changes in response to physiological events, and experimental conditions that can influence membrane characteristics or channel activity. T-type Ca^{2+} current has not been readily observed in eggs at their measured

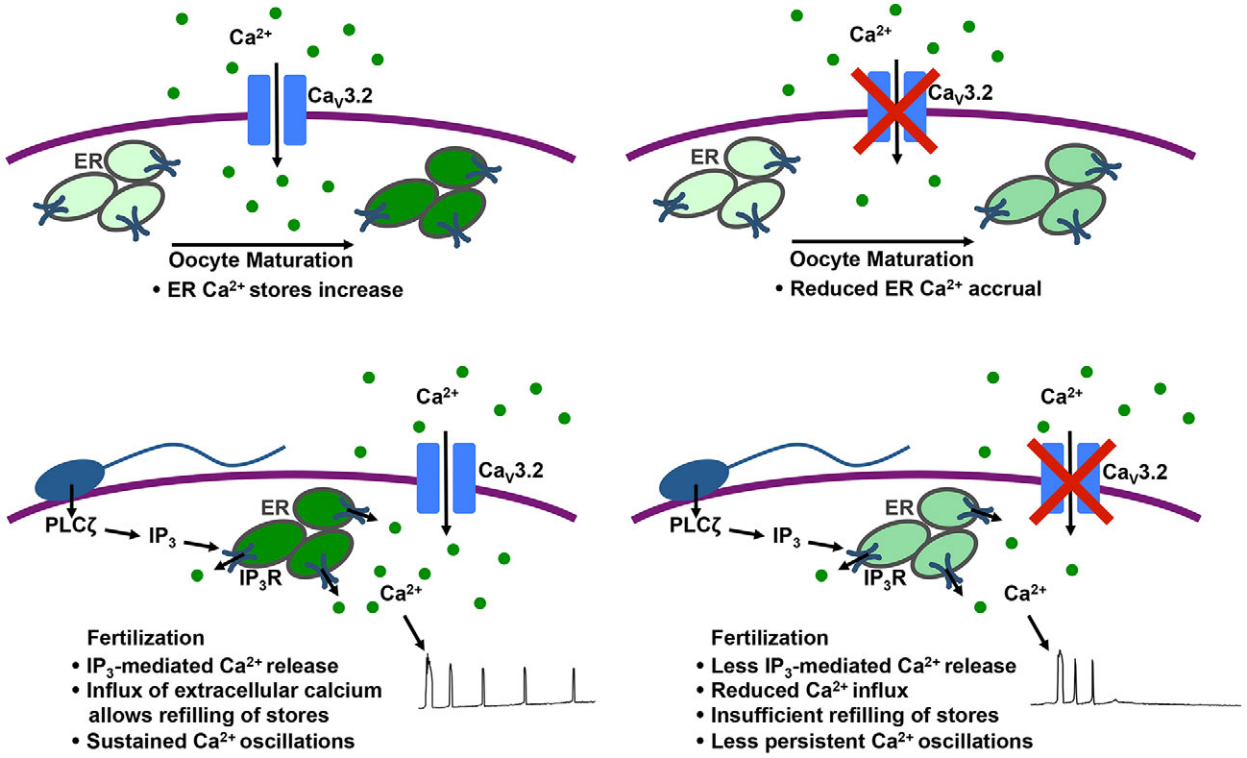

Fig. 7. Schematic showing role of $Ca_V3.2$ Ca^{2+} channels during oocyte maturation and after fertilization. Upper images: $Ca_V3.2$ channels mediate Ca^{2+} accrual during oocyte maturation. Lower images: $Ca_V3.2$ channels mediate Ca^{2+} influx needed to support sustained Ca^{2+} oscillations following fertilization. Intensity of green color indicates relative ER Ca^{2+} level. ER, endoplasmic reticulum; IP_3R, IP_3 receptor; PLCζ, phospholipase C zeta.

Journal of Cell Science (2015) 128, 4442-4452 doi:10.1242/jcs.180026

resting membrane potential, and complete inactivation of T-type channels in physiological Ca^{2+} occurs around −30 mV or −40 mV (Peres, 1986, 1987). Similarly, we found that the $Ca_V3.2$ current inactivated completely at voltages more positive than −40 mV in mouse eggs (C.F.E. and M.L.B., unpublished data). Therefore, we would expect slightly more negative membrane potentials to be required to support window currents. Membrane potentials reported here between −29 to −37 mV did not take junction potential into account; thus, true potentials might be roughly 15 mV more negative (Peres, 1987), which would put the resting membrane potential at −44 to −52 mV, within the range of window current activity. Following fertilization, gradual membrane hyperpolarization from −35 to −57 mV occurs (Igusa et al., 1983), and voltage-gated Ca^{2+} current increases (Yamashita, 1982); therefore, window currents could become more likely over time. A similar mechanism might mediate Ca^{2+} influx during oocyte maturation; resting membrane potential of germinal vesicle oocytes held at prophase I is more hyperpolarized than that of MII eggs, at −51 mV (Powers, 1982). Previous studies showing absence of substantial membrane potential changes following fertilization of mouse eggs were performed using sharp electrodes (Igusa et al., 1983; Jaffe et al., 1983), which have the potential to disrupt normal cellular physiology. Protease treatment is often used to remove the zona pellucida to facilitate patch clamping, which we suspect could alter local charge characteristics of the plasma membrane. Of note, BSA increases T-type current and shifts the voltage dependence of channel inactivation in spermatogenic cells (Espinosa et al., 2000); thus, extracellular proteins might also impact channel activity and the voltage range at which window currents are possible. Further work will be necessary to precisely define how $Ca_V3.2$ channel activity is controlled.

Herein, we provide evidence to support an essential role for the T-type Ca^{2+} channel $Ca_V3.2$ in facilitating Ca^{2+} influx in mouse oocytes and eggs to maintain Ca^{2+} homeostasis, establish appropriate ER Ca^{2+} stores, and mediate Ca^{2+} entry following fertilization to ensure activation of embryo development. These findings document an important and previously unrecognized function of a T-type channel in oocytes and eggs and outline a crucial impact of voltage-activated channels in non-excitable cells. These results have implications for laboratory procedures utilized during assisted reproduction for infertile couples and raise the possibility that therapeutic use of Ca^{2+} channel blockers in women could impact upon fertility.

MATERIALS AND METHODS

Chemicals and reagents

Leibovitz L-15 medium (L-15), alpha minimal essential medium (aMEM), AlbuMax I lipid rich bovine serum albumin (BSA), fura-2 AM and pluronic F-127 were obtained from Life Technologies. Potassium simplex optimized medium (KSOM) with amino acids and with or without BSA, human tubal fluid (HTF), Cell-Tak, PMSG and human chorionic gonadotropin (hCG) were purchased from EMD Millipore. Ca^{2+}- and Mg^{2+}-free KSOM and CZB media without BSA or polyvinyl alcohol were prepared in-house (Chatot et al., 1989; Nagy, 2003). GSK1349571A was a gift from Malcolm Begg, GlaxoSmithKline. Calf serum was from Atlanta Biologicals. Milrinone, mibefradil, pimozide, thaspigargin, ionomycin and other chemicals and reagents not specifically mentioned were from Sigma-Aldrich.

Mice

Cacna1h$^{-/-}$ mice (Chen et al., 2003), C57BL/6J males, and B6SJLF1 males were obtained from Jackson Laboratories. CF-1 female mice were from Charles River (Wilmington, MA). 6–12-week-old females were injected with 5 IU PMSG and were killed by CO_2 asphyxiation 44–48 h later for collection of germinal-vesicle-stage oocytes. For MII egg collection, mice were injected with 5 IU hCG 46–48 h after PMSG and killed 13–14 h later. All animal work was performed in accordance with National Institutes of Health and National Institute of Environmental Health Sciences guidelines under approved animal care and use protocols.

RNA isolation and real-time PCR

Triplicate samples of 50 germinal vesicle oocytes or MII eggs were collected from female CF-1 mice. 10 pg of EGFP cRNA was added to each sample prior to RNA isolation as an internal control; cRNA was *in vitro* transcribed as previously described (Miao et al., 2012). RNA was isolated using the Arcturus PicoPure RNA Isolation Kit (Life Technologies), and real time RT-PCR was performed essentially as previously described (Jefferson et al., 2013) using cDNA from 2.5 oocytes or embryos per reaction and the primers listed in Table S1. Each primer set was used to amplify the same set of cDNA samples to allow a direct comparison of relative levels. Threshold cycle (C_t) values are presented; in general, transcripts with C_t<30 were considered to have moderate-to-high expression and those with C_t<34 were considered to have low-to-moderate expression. The efficacy of primer pairs for transcripts not detected in oocytes or eggs was verified by amplifying cDNA from positive control mouse tissues, including brain, bone marrow and spleen.

Gamete collection, IVF and Ca^{2+} imaging

MII eggs were collected from oviducts of superovulated mice and treated briefly with 0.03% hyaluronidase in L-15 medium to facilitate removal of cumulus cells. For IVF experiments, zonae pellucidae were removed using acidic Tyrode's solution pH 1.6 (Nagy, 2003), and eggs were loaded with 10 µM fura-2 AM for 30 min in KSOM medium with 0.04% pluronic F-127. Caudae epididymides and vasa deferentia were dissected from 2–6-month-old B6SJLF1 males, placed in 900 µl HTF with 3 mg/ml BSA under oil, and slits were made in tissue to allow sperm to swim out for 10 min at 37°C with 5% CO_2. Concentrated sperm were diluted approximately 1:7 into the bottom of a tube of HTF with 3 mg/ml BSA and allowed to swim up and capacitate for at least 1 h. Solution from the top half of the tube, containing motile sperm, was carefully transferred to a pre-warmed tube and sperm concentration was determined using a hemocytometer. Eggs were adhered to Cell-Tak-treated glass-bottom dishes in 90 µl BSA-free KSOM, and sperm were added to a final concentration of 10^5 sperm/ml, along with 4 µl HTF containing 30 mg/ml BSA for a final concentration of ~1.5 mg/ml BSA. Imaging began immediately after sperm addition and was performed essentially as previously described (Miao et al., 2012). For low-Ca^{2+} IVF experiments, Ca^{2+}- and Mg^{2+}-free CZB medium with 0.5 mM $CaCl_2$ added was used in place of BSA-free KSOM, and insemination was performed using 5×10^4 sperm/ml. Eggs of each genotype were imaged at the same time, in the same medium drop, for each experimental replicate. For analysis of Ca^{2+} oscillations, the length of the first Ca^{2+} transient was measured as the length of time the Ca^{2+} level was at least 50% of the peak amplitude. Oscillation frequency was calculated by dividing the number of oscillations subsequent to the first transient by the time from the end of the first transient to the end of the last transient within the 60-min imaging period. Each egg was scored for persistence of oscillations to the end of the 60-min imaging period. All fertilization experiments included for analysis were performed between 14.5–17.5 h after hCG injection. For some experiments, 2 µM GSK1349571A, 10 µM mibefradil, or 5 µM pimozide was added to fertilization drops before transfer of eggs to the dish. For pimozide experiments, eggs were also pre-incubated with inhibitor during fura-2 loading, and for both mibefradil and pimozide experiments eggs were incubated for 15–30 min in BSA-free medium containing inhibitors prior to adding sperm to the fertilization drop. Control eggs for these experiments were incubated in BSA-free medium with equivalent concentrations of DMSO or water vehicle. For mibefradil experiments, fourfold more sperm were added to drops containing mibefradil versus control medium (2×10^5 and 5×10^4 sperm/ml, respectively) to compensate for partial impairment of sperm motility or fertilizing ability caused by mibefradil (Darszon et al., 2006) and to achieve a more similar rate and timing of fertilization. For assessment of polyspermy, eggs were washed in HTF to remove unfused sperm 1 h after insemination and were fixed and mounted as previously described (Bernhardt et al., 2011).

Electrophysiology

Experiments were performed using conditions similar to those previously described (Peres, 1987). Briefly, currents were measured with an EPC10 patch-clamp amplifier in combination with PatchMaster software (HEKA

Instruments, Holliston, MA) for data acquisition and analysis. Pipette solution contained (in mM): 140 CsCl, 10 2-[4-(2-hydroxyethyl)piperazin-1-yl]ethanesulfonic acid (HEPES), 1 1,2-bis(o-aminophenoxy)ethane-N,N,N′,N′-tetraacetic acid (BAPTA), 0.1 $CaCl_2$, 2 $MgCl_2$, adjusted to pH 7.2 with tetraethylammonium-hydroxide (TEA-OH), and external solution contained (in mM): 125 NaCl, 20 HEPES, 6 KCl, 1.7 or 20 $CaCl_2$, adjusted to pH 7.5 with NaOH. Cumulus-free superovulated eggs were treated with 0.5% (w/v) pronase in L-15 medium for 4–8 min to remove zonae pellucidae. Pipettes with resistance of 3–5 MΩ were used, and whole-cell patch clamps were established in external solution containing 20 mM Ca^{2+} to facilitate seal formation; typical seals of 1–5 GΩ were achieved prior to breaking into cells. The pipette series resistance (Rs) was electronically compensated, typically by ∼70%. Linear leak and capacitive currents were subtracted by the P/4 procedure using PatchMaster software. Currents were expressed as current density (pA/pF) rather than absolute currents to account for any difference in oocyte size. Experiments were performed at ambient room temperature. Eggs were held at −80 mV, and 50-ms duration depolarizing steps from −70 mV to +50 mV in 10 mV increments were applied at 5 s intervals. For *Cacna1h*$^{+/+}$, *Cacna1h*$^{+/-}$, and *Cacna1h*$^{-/-}$ eggs, measurements were performed in solution containing 20 mM Ca^{2+}. For experiments using inhibitors, seals were achieved in 20 mM Ca^{2+} solution followed by equilibration in 1.7 mM Ca^{2+} and baseline measurements before beginning perfusion with solutions containing inhibitors. For determination of the resting membrane potential, a potassium-based pipette solution was used with (in mM): 150 KCl, 1 ethylene glycol tetraacetic acid (EGTA), 10 HEPES, 2 MgATP, 0.2 NaGTP, 0.2 $CaCl_2$, adjusted to pH 7.2 with KOH. The resting potential was determined by switching from voltage- to current-clamp after breaking into the cell and stabilization of the holding current.

Oocyte collection and IVM

Germinal vesicle oocytes were collected essentially as previously described (Bernhardt et al., 2011). 10 µM milrinone was added to collection medium to prevent meiotic resumption, and cumulus cells were removed prior to *in vitro* maturation (IVM) culture. Oocytes were matured in aMEM with 5% calf serum for 14–17.5 h (37°C and 5% CO_2), with addition of vehicle, 1, 5 or 10 µM milrinone, or 0.5, 2 or 5 µM pimozide, as indicated. Culture with inhibitors was performed in 0.5 ml medium without oil overlay, and inhibitors were included in fura-2-AM-loading drops where appropriate.

Ca^{2+} store and Mn^{2+}-quenching assays

For assays of total Ca^{2+} stores, fura-2-AM-loaded oocytes or eggs were adhered to glass-bottom dishes in 2 ml of Ca^{2+}- and BSA-free KSOM. Baseline ratiometric imaging was performed for 3–5 min, followed by addition of ionomycin to a final concentration of 5 µM. Additions were performed by drop-wise infusion of stock solutions diluted in 150 µl of medium, near the edge of the imaging dish. Assays of ER Ca^{2+} stores were performed similarly in Ca^{2+}- and Mg^{2+}-free CZB without BSA or polyvinyl alcohol and supplemented with 2 mM EGTA with zona-pellucida-intact oocytes or eggs; thapsigargin was added to a final concentration of 10 µM. The area under the curve measurements were calculated using trapezoidal area for baseline-subtracted curves, and the maximum amplitude was also determined relative to baseline measurements prior to ionomycin or thapsigargin addition. The area under the curve was measured for the first 5 min following the initial Ca^{2+} response for ionomycin assays and for the first 10 min for thapsigargin assays. For Mn^{2+}-quenching assays, aMEM medium containing pimozide or vehicle control was used; Mn^{2+} and ionomycin were added to final concentrations of 1 mM and 5 µM, respectively. Imaging of fluorophores at 340 nm, 380 nm and 360 nm (F340, F380 and F360, respectively) was performed using Intracellular InCyt Im3 software, on the same imaging system described above. For assays using CZB or aMEM medium, fura-2 AM loading was performed in aMEM with 5% calf serum rather than KSOM to avoid exposing cells to changes in osmolarity.

Statistical analysis

Statistical tests were performed using GraphPad Prism, version 6.0. Data were tested for normal distribution using a D'Agostino and Pearson omnibus normality test and were analyzed using a Mann–Whitney U-test, Student's *t*-test, Fisher's exact test, chi-square test, Kruskal-Wallis test, 1- or 2-way ANOVA, and appropriate post-hoc tests for multiple comparisons, as indicated in figure legends. Error bars show s.e.m. for all graphs.

Acknowledgements

We thank Jim Putney, Gary Bird, and Rindy Jaffe for helpful discussions and critical reading of the manuscript. We also thank Malcolm Begg (GlaxoSmithKline) for kindly providing the GSK1349571A compound.

Competing interests

The authors declare no competing or financial interests.

Author contributions

M.L.B., C.F.E., Y.-L.M., D.L.A. and C.J.W. designed the experiments. M.L.B., Y.Z., C.F.E., E.P.-B., C.E.M. and Y.-L.M. performed the experiments and analyzed the data. M.L.B. and C.J.W. wrote the paper, and all authors edited the paper.

Funding

This work was supported by the Intramural Research Program of the National Institutes of Health, National Institutes of Environmental Health Sciences [grant number 1ZIAES102985]. Deposited in PMC for release after 12 months.

Supplementary information

Supplementary information available online at
http://jcs.biologists.org/lookup/suppl/doi:10.1242/jcs.180026/-/DC1

References

Arnoult, C., Cardullo, R. A., Lemos, J. R. and Florman, H. M. (1996). Activation of mouse sperm T-type Ca2+ channels by adhesion to the egg zona pellucida. *Proc. Natl. Acad. Sci. USA* **93**, 13004-13009.

Arnoult, C., Villaz, M. and Florman, H. M. (1998). Pharmacological properties of the T-type Ca2+ current of mouse spermatogenic cells. *Mol. Pharmacol.* **53**, 1104-1111.

Backs, J., Stein, P., Backs, T., Duncan, F. E., Grueter, C. E., McAnally, J., Qi, X., Schultz, R. M. and Olson, E. N. (2010). The gamma isoform of CaM kinase II controls mouse egg activation by regulating cell cycle resumption. *Proc. Natl. Acad. Sci. USA* **107**, 81-86.

Bernhardt, M. L., Kim, A. M., O'Halloran, T. V. and Woodruff, T. K. (2011). Zinc requirement during meiosis I-meiosis II transition in mouse oocytes is independent of the MOS-MAPK pathway. *Biol. Reprod.* **84**, 526-536.

Bird, G. S., DeHaven, W. I., Smyth, J. T. and Putney, J. W., Jr. (2008). Methods for studying store-operated calcium entry. *Methods* **46**, 204-212.

Capiod, T. (2011). Cell proliferation, calcium influx and calcium channels. *Biochimie* **93**, 2075-2079.

Chatot, C. L., Ziomek, C. A., Bavister, B. D., Lewis, J. L. and Torres, I. (1989). An improved culture medium supports development of random-bred 1-cell mouse embryos in vitro. *J. Reprod. Fertil.* **86**, 679-688.

Chemin, J., Monteil, A., Briquaire, C., Richard, S., Perez-Reyes, E., Nargeot, J. and Lory, P. (2000). Overexpression of T-type calcium channels in HEK-293 cells increases intracellular calcium without affecting cellular proliferation. *FEBS Lett.* **478**, 166-172.

Chen, C. C., Lamping, K. G., Nuno, D. W., Barresi, R., Prouty, S. J., Lavoie, J. L., Cribbs, L. L., England, S. K., Sigmund, C. D., Weiss, R. M. et al. (2003). Abnormal coronary function in mice deficient in alpha1H T-type Ca2+ channels. *Science* **302**, 1416-1418.

Cheon, B., Lee, H.-C., Wakai, T. and Fissore, R. A. (2013). Ca2+ influx and the store-operated Ca2+ entry pathway undergo regulation during mouse oocyte maturation. *Mol. Biol. Cell* **24**, 1396-1410.

Darszon, A., López-Marínez, P., Acevedo, J. J., Hernandez-Cruz, A. and Trevino, C. L. (2006). T-type Ca2+ channels in sperm function. *Cell Calcium* **40**, 241-252.

Day, M. L., Johnson, M. H. and Cook, D. I. (1998). Cell cycle regulation of a T-type calcium current in early mouse embryos. *Pflugers Arch.* **436**, 834-842.

Ducibella, T. and Fissore, R. (2008). The roles of Ca2+, downstream protein kinases, and oscillatory signaling in regulating fertilization and the activation of development. *Dev. Biol.* **315**, 257-279.

Espinosa, F., López-Gonzólez, I., Muñoz-Garay, C., Felix, R., De la Vega-Beltrán, J. L., Kopf, G. S., Visconti, P. E. and Darszon, A. (2000). Dual regulation of the T-type Ca(2+) current by serum albumin and beta-estradiol in mammalian spermatogenic cells. *FEBS Lett.* **475**, 251-256.

Fissore, R. A., Longo, F. J., Anderson, E., Parys, J. B. and Ducibella, T. (1999). Differential distribution of inositol trisphosphate receptor isoforms in mouse oocytes. *Biol. Reprod.* **60**, 49-57.

FitzHarris, G., Marangos, P. and Carroll, J. (2007). Changes in endoplasmic reticulum structure during mouse oocyte maturation are controlled by the cytoskeleton and cytoplasmic dynein. *Dev. Biol.* **305**, 133-144.

Gallo, A., Russo, G. L. and Tosti, E. (2013). T-type Ca2+ current activity during oocyte growth and maturation in the ascidian Styela plicata. *PLoS ONE* **8**, e54604.

Gomez-Fernandez, C., Pozo-Guisado, E., Ganan-Parra, M., Perianes, M. J., Alvarez, I. S. and Martin-Romero, F. J. (2009). Relocalization of STIM1 in mouse oocytes at fertilization: early involvement of store-operated calcium entry. *Reproduction* **138**, 211-221.
Gomez-Fernandez, C., Lopez-Guerrero, A. M., Pozo-Guisado, E., Alvarez, I. S. and Martin-Romero, F. J. (2012). Calcium signaling in mouse oocyte maturation: the roles of STIM1, ORAI1 and SOCE. *Mol. Hum. Reprod.* **18**, 194-203.
Gould-Somero, M., Jaffe, L. A. and Holland, L. Z. (1979). Electrically mediated fast polyspermy block in eggs of the marine worm, Urechis caupo. *J. Cell Biol.* **82**, 426-440.
Homa, S. T., Carroll, J. and Swann, K. (1993). The role of calcium in mammalian oocyte maturation and egg activation. *Hum. Reprod.* **8**, 1274-1281.
Igusa, Y. and Miyazaki, S. (1983). Effects of altered extracellular and intracellular calcium concentration on hyperpolarizing responses of the hamster egg. *J. Physiol.* **340**, 611-632.
Igusa, Y., Miyazaki, S.-i. and Yamashita, N. (1983). Periodic hyperpolarizing responses in hamster and mouse eggs fertilized with mouse sperm. *J. Physiol.* **340**, 633-647.
Jaffe, L. A., Sharp, A. P. and Wolf, D. P. (1983). Absence of an electrical polyspermy block in the mouse. *Dev. Biol.* **96**, 317-323.
Jagiello, G., Ducayen, M. B., Downey, R. and Jonassen, A. (1982). Alterations of mammalian oocyte meiosis I with divalent cations and calmodulin. *Cell Calcium* **3**, 153-162.
Jefferson, W. N., Chevalier, D. M., Phelps, J. Y., Cantor, A. M., Padilla-Banks, E., Newbold, R. R., Archer, T. K., Kinyamu, H. K. and Williams, C. J. (2013). Persistently altered epigenetic marks in the mouse uterus after neonatal estrogen exposure. *Mol. Endocrinol.* **27**, 1666-1677.
Kang, D., Hur, C.-G., Park, J.-Y., Han, J. and Hong, S.-G. (2007). Acetylcholine increases Ca2+ influx by activation of CaMKII in mouse oocytes. *Biochem. Biophys. Res. Commun.* **360**, 476-482.
Kashir, J., Deguchi, R., Jones, C., Coward, K. and Stricker, S. A. (2013). Comparative biology of sperm factors and fertilization-induced calcium signals across the animal kingdom. *Mol. Reprod. Dev.* **80**, 787-815.
Kashir, J., Nomikos, M., Lai, F. A. and Swann, K. (2014). Sperm-induced Ca2+ release during egg activation in mammals. *Biochem. Biophys. Res. Commun.* **450**, 1204-1211.
Kline, D. and Kline, J. T. (1992a). Repetitive calcium transients and the role of calcium in exocytosis and cell cycle activation in the mouse egg. *Dev. Biol.* **149**, 80-89.
Kline, D. and Kline, J. T. (1992b). Thapsigargin activates a calcium influx pathway in the unfertilized mouse egg and suppresses repetitive calcium transients in the fertilized egg. *J. Biol. Chem.* **267**, 17624-17630.
Knott, J. G., Gardner, A. J., Madgwick, S., Jones, K. T., Williams, C. J. and Schultz, R. M. (2006). Calmodulin-dependent protein kinase II triggers mouse egg activation and embryo development in the absence of Ca2+ oscillations. *Dev. Biol.* **296**, 388-395.
Kuryshev, Y. A., Brown, A. M., Duzic, E. and Kirsch, G. E. (2014). Evaluating state dependence and subtype selectivity of calcium channel modulators in automated electrophysiology assays. *Assay Drug Dev. Technol.* **12**, 110-119.
Lee, K., Wang, C. and Machaty, Z. (2012). STIM1 is required for Ca2+ signaling during mammalian fertilization. *Dev. Biol.* **367**, 154-162.
Machaca, K. and Haun, S. (2002). Induction of maturation-promoting factor during Xenopus oocyte maturation uncouples Ca(2+) store depletion from store-operated Ca(2+) entry. *J. Cell Biol.* **156**, 75-86.
Markoulaki, S., Matson, S., Abbott, A. L. and Ducibella, T. (2003). Oscillatory CaMKII activity in mouse egg activation. *Dev. Biol.* **258**, 464-474.
Martin, R. L., Lee, J. H., Cribbs, L. L., Perez-Reyes, E. and Hanck, D. A. (2000). Mibefradil block of cloned T-type calcium channels. *J. Pharmacol. Exp. Ther.* **295**, 302-308.
McGuinness, O. M., Moreton, R. B., Johnson, M. H. and Berridge, M. J. (1996). A direct measurement of increased divalent cation influx in fertilised mouse oocytes. *Development* **122**, 2199-2206.
Mehlmann, L. M., Terasaki, M., Jaffe, L. A. and Kline, D. (1995). Reorganization of the endoplasmic reticulum during meiotic maturation of the mouse oocyte. *Dev. Biol.* **170**, 607-615.
Mehlmann, L. M., Mikoshiba, K. and Kline, D. (1996). Redistribution and increase in cortical inositol 1,4,5-trisphosphate receptors after meiotic maturation of the mouse oocyte. *Dev. Biol.* **180**, 489-498.
Miao, Y.-L. and Williams, C. J. (2012). Calcium signaling in mammalian egg activation and embryo development: the influence of subcellular localization. *Mol. Reprod. Dev.* **79**, 742-756.
Miao, Y.-L., Stein, P., Jefferson, W. N., Padilla-Banks, E. and Williams, C. J. (2012). Calcium influx-mediated signaling is required for complete mouse egg activation. *Proc. Natl. Acad. Sci. USA* **109**, 4169-4174.
Miyazaki, S.-I., Hashimoto, N., Yoshimoto, Y., Kishimoto, T., Igusa, Y. and Hiramoto, Y. (1986). Temporal and spatial dynamics of the periodic increase in intracellular free calcium at fertilization of golden hamster eggs. *Dev. Biol.* **118**, 259-267.
Nagy, A. (2003). *Manipulating the Mouse Embryo: A Laboratory Manual*. Cold Spring Harbor, N.Y: Cold Spring Harbor Laboratory Press.
Ozil, J.-P., Markoulaki, S., Toth, S., Matson, S., Banrezes, B., Knott, J. G., Schultz, R. M., Huneau, D. and Ducibella, T. (2005). Egg activation events are regulated by the duration of a sustained [Ca2+]cyt signal in the mouse. *Dev. Biol.* **282**, 39-54.
Ozil, J.-P., Banrezes, B., Tóth, S., Pan, H. and Schultz, R. M. (2006). Ca2+ oscillatory pattern in fertilized mouse eggs affects gene expression and development to term. *Dev. Biol.* **300**, 534-544.
Peres, A. (1986). Resting membrane potential and inward current properties of mouse ovarian oocytes and eggs. *Pflugers Arch.* **407**, 534-540.
Peres, A. (1987). The calcium current of mouse egg measured in physiological calcium and temperature conditions. *J. Physiol.* **391**, 573-588.
Powers, R. D. (1982). Changes in mouse oocyte membrane potential and permeability during meiotic maturation. *J. Exp. Zool.* **221**, 365-371.
Putney, J. W.Jr. (1986). A model for receptor-regulated calcium entry. *Cell Calcium* **7**, 1-12.
Putney, J. W., Jr. (2007). Recent breakthroughs in the molecular mechanism of capacitative calcium entry (with thoughts on how we got here). *Cell Calcium* **42**, 103-110.
Runft, L. L., Jaffe, L. A. and Mehlmann, L. M. (2002). Egg activation at fertilization: where it all begins. *Dev. Biol.* **245**, 237-254.
Saunders, C. M., Larman, M. G., Parrington, J., Cox, L. J., Royse, J., Blayney, L. M., Swann, K. and Lai, F. A. (2002). PLC zeta: a sperm-specific trigger of Ca(2+) oscillations in eggs and embryo development. *Development* **129**, 3533-3544.
Schultz, R. M. and Kopf, G. S. (1995). Molecular basis of mammalian egg activation. *Curr. Top. Dev. Biol.* **30**, 21-62.
Serrano, J. R., Perez-Reyes, E. and Jones, S. W. (1999). State-dependent inactivation of the alpha1G T-type calcium channel. *J. Gen. Physiol.* **114**, 185-202.
Smyth, J. T., Petranka, J. G., Boyles, R. R., DeHaven, W. I., Fukushima, M., Johnson, K. L., Williams, J. G. and Putney, J. W., Jr. (2009). Phosphorylation of STIM1 underlies suppression of store-operated calcium entry during mitosis. *Nat. Cell Biol.* **11**, 1465-1472.
Stricker, S. A. (1999). Comparative biology of calcium signaling during fertilization and egg activation in animals. *Dev. Biol.* **211**, 157-176.
Takahashi, T., Kikuchi, T., Kidokoro, Y. and Shirakawa, H. (2013). Ca(2+) influx-dependent refilling of intracellular Ca(2+) stores determines the frequency of Ca(2+) oscillations in fertilized mouse eggs. *Biochem. Biophys. Res. Commun.* **430**, 60-65.
Tombes, R. M., Simerly, C., Borisy, G. G. and Schatten, G. (1992). Meiosis, egg activation, and nuclear envelope breakdown are differentially reliant on Ca2+, whereas germinal vesicle breakdown is Ca2+ independent in the mouse oocyte. *J. Cell Biol.* **117**, 799-811.
Wakai, T. and Fissore, R. A. (2013). Ca(2+) homeostasis and regulation of ER Ca(2+) in mammalian oocytes/eggs. *Cell Calcium* **53**, 63-67.
Wang, C., Lee, K., Gajdócsi, E., Papp, Á. B. and Machaty, Z. (2012). Orai1 mediates store-operated Ca2+ entry during fertilization in mammalian oocytes. *Dev. Biol.* **365**, 414-423.
Wang, C., Zhang, L., Jaeger, L. A. and Machaty, Z. (2015). Store-operated Ca2+ entry sustains the fertilization Ca2+ signal in pig eggs. *Biol. Reprod.* **93**, 25.
Watari, H., Tose, A. J. and Bosma, M. M. (2014). Looping circuit: a novel mechanism for prolonged spontaneous [Ca2+]i increases in developing embryonic mouse brainstem. *J. Physiol.* **592**, 711-727.
Williams, S. R., Tóth, T. I., Turner, J. P., Hughes, S. W. and Crunelli, V. (1997). The 'window' component of the low threshold Ca2+ current produces input signal amplification and bistability in cat and rat thalamocortical neurones. *J. Physiol.* **505**, 689-705.
Williams, M. E., Washburn, M. S., Hans, M., Urrutia, A., Brust, P. F., Prodanovich, P., Harpold, M. M. and Stauderman, K. A. (1999). Structure and functional characterization of a novel human low-voltage activated calcium channel. *J. Neurochem.* **72**, 791-799.
Yamashita, N. (1982). Enhancement of ionic currents through voltage-gated channels in the mouse oocyte after fertilization. *J. Physiol.* **329**, 263-280.
Zhang, Y., Jiang, X., Snutch, T. P. and Tao, J. (2013). Modulation of low-voltage-activated T-type Ca(2+) channels. *Biochim. Biophys. Acta* **1828**, 1550-1559.